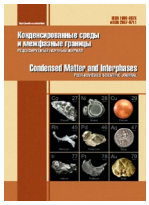

ISSN 1606-867X (Print)
ISSN 2687-0711 (Online)
Condensed Matter and Interphases
Kondensirovannye Sredy i Mezhfaznye Granitsy
https://journals.vsu.ru/kcmf/

Original articles

Research article
https://doi.org/10.17308/kcmf.2025.27/12487

Refinement of the phase diagram of the MnSe–In_2Se_3 system and the crystal structures of $MnIn_2Se_4$ and $Mn_2In_2Se_5$ compounds

F. M. Mammadov[1,2]✉, S. Z. Imamaliyeva[1], E. N. Ismailova[1], I. R. Amiraslanov[3], E. I. Akhmedov[4], M. B. Babanly[1,4]

[1]*Institute of Catalysis and Inorganic Chemistry, 113 H. Javid av., Baku AZ-1143, Azerbaijan*

[2]*Pedagogical University, 68 Uzeyir Hajibeyov st., Baku AZ-1000, Azerbaijan*

[3]*Institute of Physics of Azerbaijan National Academy of Sciences, 131 G. Javid ave., Baku AZ-1143, Azerbaijan*

[4]*Baku State University, 23 Z. Khalilov st., Baku AZ-1148, Azerbaijan*

Abstract

Complex chalcogenides based on transition elements, in particular ternary compounds of the AB_2X_4 type (M = Mn, Fe, Co, Ni; B = Ga, In, Sb, Bi; X = S, Se, Te) are among the important functional materials. Compounds of this class exhibit the phenomena of electronically or optically controlled magnetism and are very promising for the creation of lasers, light modulators, photodetectors, and other functional devices controlled by a magnetic field. Recent studies demonstrated that these compounds can also find application in photocatalysis, photovoltaics, and thermoelectric converters.

The study presents new data on phase equilibria in the MnSe–In_2Se_3 system, obtained by differential thermal analysis, X-ray phase analysis, and scanning electron microscopy. Two ternary compounds, $MnIn_2Se_4$ with congruent melting at 1193 K and $Mn_2In_2Se_5$, melting incongruently at 1196 K, were formed in the system. The first is a phase of variable composition and has a 5–6 mol. % homogeneity region towards an excess of In_2Se_3. Based on powder diffraction data, the Rietveld method was used to refine the crystal structures and lattice parameters of both ternary compounds.

Keywords: Manganese-indium selenides, Phase equilibria, Homogeneity region, Crystal structure, Rietveld method

Funding: This work is supported by the Azerbaijan Science Foundation – Grant No AEF-MCG-2022-1(42)-12/10/4-M-10.

For citation: Mammadov F. M., Imamaliyeva S. Z., Ismailova E. N., Amiraslanov I. R., Akhmedov E. I., Babanly M. B. Refinement of the phase diagram of the MnSe–In_2Se_3 system and the crystal structures of $MnIn_2Se_4$ and $Mn_2In_2Se_5$ compounds. *Condensed Matter and Interphases.* 2025;27(1): 57–66. https://doi.org/10.17308/kcmf.2025.27/12487

Для цитирования: Мамедов Ф. М., Имамалиева С. З., Исмаилова Э. Н., Амирасланов И. Р., Ахмедов Э. И., Бабанлы М. Б. Уточнение фазовой диаграммы системы MnSe–In_2Se_3 и кристаллических структур соединений $MnIn_2Se_4$ и $Mn_2In_2Se_5$. *Конденсированные среды и межфазные границы*. 2025;27(1): 57–66. https://doi.org/10.17308/kcmf.2025.27/12487

✉ Faik M. Mammadov, e-mail: faikmamadov@mail.ru

1. Introduction

Complex transition metal chalcogenides, in particular compounds of the AB_2X_4 and $A_2B_2X_5$ types (A = Fe, Mn, Co; B = Al, Ga, In, Sb, Bi; X = S, Se, Te) with a layered structure are among the important materials possessing thermoelectric [1, 2], magnetic [3–9], optical, and other functional properties [10–13]. This makes them very promising for use in the creation of lasers, light modulators, photodetectors, thermoelectric, and other functional devices. In addition, they are objects of intensive research as magnetic topological insulators, combining the properties of an antiferromagnet and a topological insulator, and are extremely promising for use in spintronics, quantum computing, and information processing devices [14–22].

A number of recent studies have shown that some compounds of the AB_2X_4 type and heterojunctions based on them can find application in photocatalysis and photovoltaics, in particular, in photocatalytic water splitting [23–27]. According to the results of [28–30], some compounds of the above type with a spinel structure are good candidates for use as a new type of anode materials for the stable storage of ions in lithium (sodium) ion batteries.

The results described above show the relevance of research aimed at obtaining and studying the properties of new complex layered chalcogenides of transition elements. Modification of such compounds by alloying and obtaining solid solutions can be used to optimize their functional properties [31–36].

The development of methods for the targeted synthesis of complex chalcogenide compounds and phases of variable composition is based on data of phase equilibria in the corresponding systems. Phase diagrams provide valuable information on the nature of formation, thermal stability, phase transformations, primary crystallization regions, and the homogeneity of intermediate phases [37–43].

Previously, studies of phase equilibria in a number of quasi-ternary $MX–Ga_2X_3–In_2X_3$ systems (M = Mn, Fe; X = S, Se, Te) were performed, in search of the physicochemical foundations for creating new magnetic semiconductors [44–50]. In the indicated systems, new phases of variable composition based on ternary AB_2X_4 compounds have been identified, their primary crystallization fields and homogeneity regions were determined.

Preliminary experimental results in the study of the MnSe–Ga_2Se_3–In_2Se_3 system, revealed their discrepancy with the known [51] phase diagram of the MnSe–In_2Se_3 boundary system. Taking this into account these findings, in this study we have undertaken a repeated study of phase equilibria in the MnSe–In_2Se_3system.

The initial compounds of the studied system were investigated in detail. The MnSe compound melts congruently at 1875 K and has three modifications: a stable low-temperature α-MnSe crystallizes in a cubic NaCl-type structure. The β-MnSe and γ-MnSe phases are unstable. The first phase crystallizes in a cubic structure of the sphalerite type, and the second crystallizes in a hexagonal structure of the wurtzite type [52–55], (Table 1).

The In_2Se_3 compound melts with an open maximum at 1158 K and undergoes three polymorphic transformations (473, 920, and 1023 K) [52, 53]. The types and parameters of crystal lattices of all four crystalline modifications of In_2Se_3 are described in detail in [56], (Table 1).

Table. 1. Crystallographic data of MnSe and In_2Se_3

Соединение	Type and parameters of the crystal lattice, nm	Ref.
MnSe-rt	Kubik, Sp.Gr. $Fm\bar{3}m$; a = 0.5456	[54]
MnSe-ht1	Kubik, Sp.Gr. $F\bar{4}3m$; a = 0.583	[55]
MnSe-ht2	Heksaqonal, Sp.Gr. $P63mc$; a = 0.413, c = 0.673	[55]
In_2Se_3-rt	Heksaqonal, Sp.Gr. $R3m$; a = 0.405, c = 2.877	[56]
In_2Se_3-ht1	Heksaqonal, Sp.Gr. $P6_5$; a = 0.711, c = 1.930	[56]
In_2Se_3-ht2	Heksaqonal, Sp.Gr. $P6_1$; a = 0.7133, c = 1.934	[56]
In_2Se_3- ht3	Heksaqonal, Sp.Gr. $P6_1$; a = 0.4014, c = 0.964	[56]

2. Experimental

2.1. Synthesis

The MnSe and In_2Se_3 compounds were synthesized by the direct interaction of stoichiometric quantities of high-purity elemental components (manganese – 99.95%, indium – 99.999% and selenium – 99.99% from Alfa Aesar) in sealed quartz glass ampoules evacuated to ~ 10^{-2} Pa. The syntheses were carried out in a two-zone inclined furnace. The lower "hot" zone was heated to 1200 K, and the upper "cold" zone was heated to 900 K, which is slightly lower than the boiling point (958 K) of elemental selenium [57]. In order to avoid the interaction of quartz with manganese, MnSe synthesis was carried out in a graphitized ampoule.

The individuality of the synthesized compounds was controlled by differential thermal analysis (DTA) and X-ray diffraction (XRD) methods. Temperatures of polymorphic transitions and melting of In_2Se_3, determined based on the DTA heating curves, coincided with the available literature data [52, 53]. The following crystallographic parameters were obtained by interpretation of the powder X-ray diffraction patterns: MnSe – cubic, sp. gr. $Fm\bar{3}m$, a = 0.54542(4) nm, RT-In_2Se_3 – hexagonal, sp.gr. $R\bar{3}m$, a = 0.40804(5), c = 2.8712(14) nm, which are in good agreement with the literature data [54–56], (Table 1).

Alloys of the MnSe– In_2Se_3 system were prepared by fusing the initial binary compounds in various ratios in evacuated quartz ampoules at 1200–1300 K, followed by thermal annealing at 800 K for 500 hours and cooling in a switched-off furnace.

2.2. Research methods

The studies were carried out using DTA, X-ray diffraction and scanning electron microscopy (SEM) methods. The DTA of samples weighing 0.1–0.3 g in evacuated quartz ampoules was carried out using a Netzsch STA 449 F3 unit (platinum – platinum/rhodium thermocouples) in the temperature range from room temperature to ~ 1450 K with a heating rate of 10 K·min^{-1}. The temperature measurement accuracy was within ±2 K.

The X-ray powder diffraction analysis of powder samples was performed using a D2 Phaser diffractometer (Bruker, Germany; Cu$K\alpha$-radiation, angle range 5° ⩽ 2θ ⩽ 80°, scanning rate of 0.03°×0.2 min). The crystal lattice parameters of ternary compounds were refined by the Rietveld method using the EVA and TOPAS 4.2 programs. The SEM analysis was performed using the Tescan Vega 3 SBH scanning electron microscope.

3. Results and discussion

The joint processing of DTA, X-ray diffraction, and SEM data for synthesized and annealed alloys allowed us to obtain a new, more precise pattern of phase equilibria in the MnSe – In_2Se_3 system. Below in the text, in the figures and in the tables the following phase designations are used: α and γ-solid solutions based on the MnSe and $MnIn_2Se_4$; β_1, β_2, β_3 and β_4-solid solutions based on high-temperature, two intermediate and low-temperature modifications of the In_2Se_3 compound, respectively.

The X-ray diffraction method showed that alloys of composition 33.3 ($Mn_2In_2Se_5$) and 50 mol. % In_2Se_3 ($MnIn_2Se_4$) have individual diffraction patterns that differ from those of the original compounds. Diffraction patterns of other intermediate alloys consisted of two-phase mixtures α + $Mn_2In_2Se_5$, $Mn_2In_2Se_5$ + $MnIn_2Se_4$ (γ) and γ + β_4 respectively (Fig. 1).

Based on powder diffraction patterns, the Rietveld method was used to refine the crystal structures of both ternary compounds. The experimental and calculated diffraction patterns, as well as the differences in their intensities are shown in Fig. 2 and 3. The refined parameters of the elementary cells are shown in Table 2, and the atomic positional parameters are shown in Tables 3 and 4. The crystal structures of the $MnIn_2Se_4$ and $Mn_2In_2Se_5$ compounds are shown in Fig. 4. Both compounds are layered phases of the van der Waals type. Their structural blocks are fragments consisting of 7 and 9 atomic layers, in which the atoms alternate as Se-In-Se-Mn-Se-In-Se and Se-In-Se-Mn-Se-Mn-Se-In-Se respectively. In both structures, Mn atoms are located at the centers of octahedra, and In atoms are located at the centers of tetrahedra formed by Se atoms. These blocks are bound together by van der Waals bonds. The results obtained for polycrystalline samples using the Rietveld method are in good agreement with the data of studies [58, 59], obtained based on diffraction data of single crystals.

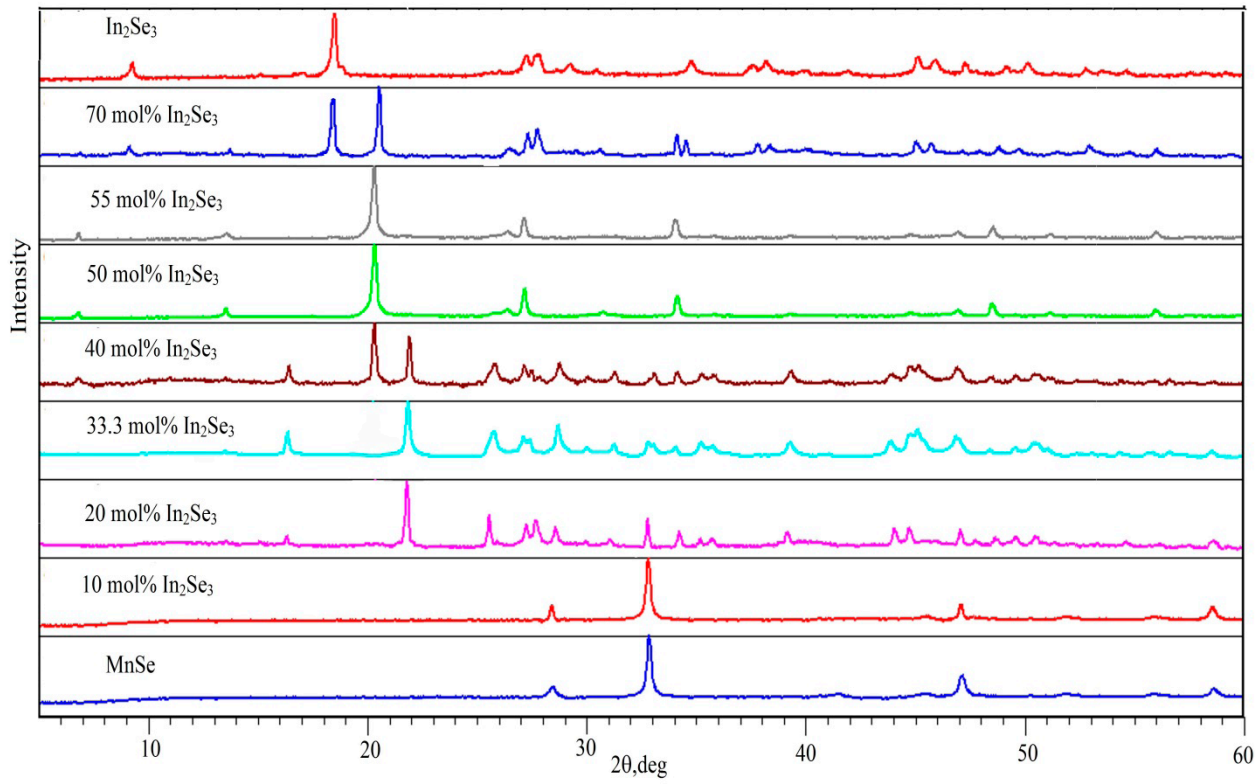

Fig. 1. The XRD patterns of alloys of the MnSe-In_2Se_3 system

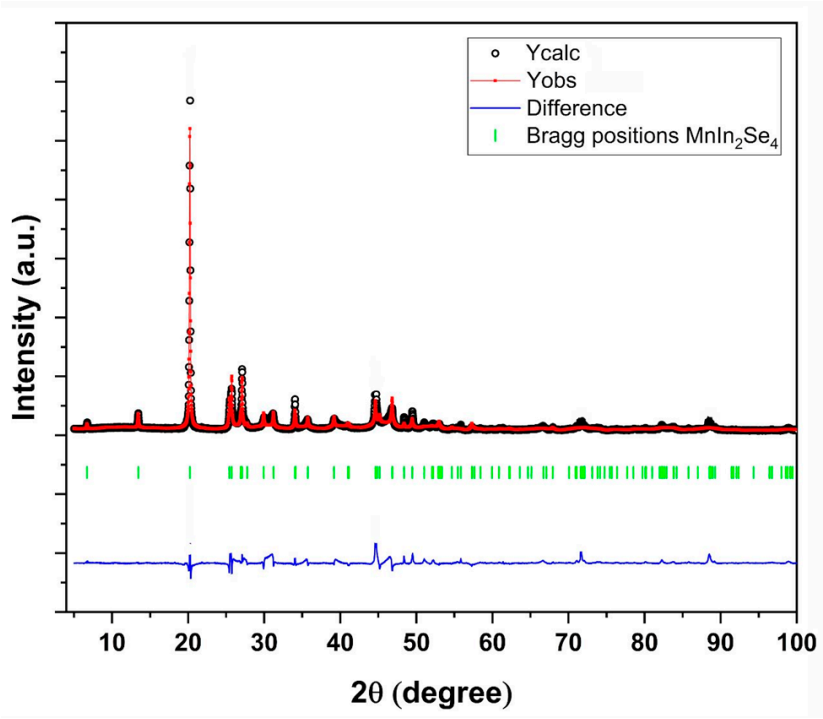

Fig. 2. Experimental and calculated diffraction lines of $MnIn_2Se_4$, as well as the differences in their intensities

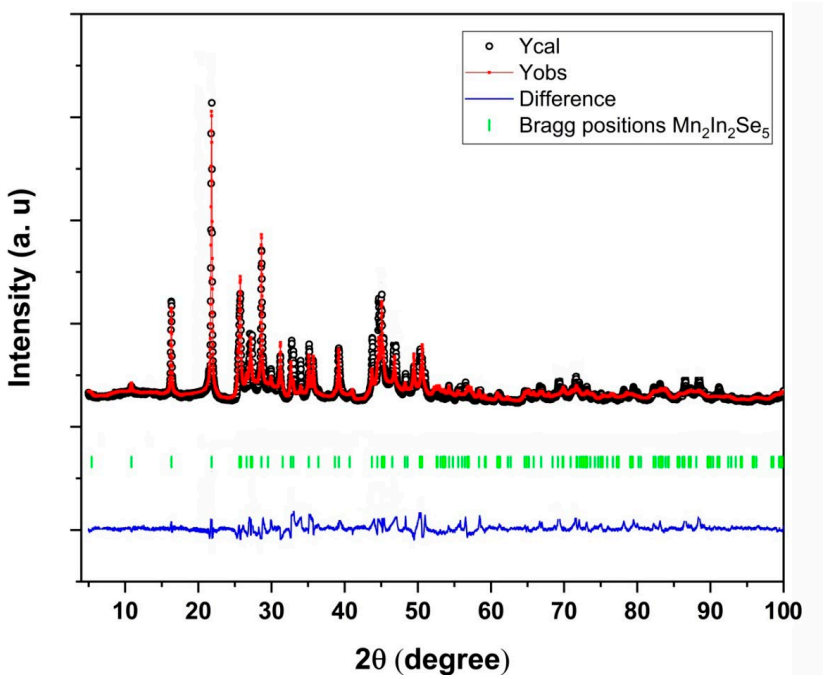

Fig. 3. Experimental and calculated diffraction lines of $Mn_2In_2Se_5$, as well as the differences in their intensities

Table. 2. Refined parameters of the structure of $MnIn_2Se_4$ and $Mn_2In_2Se_5$

Structure parameters	$MnIn_2Se_4$	$Mn_2In_2Se_5$
Space group	$R\bar{3}m$	$R\bar{3}m$
Cell parameters: *a* (nm) *c* (nm)	 0.405289(45) 3.94594(44)	 0. 402240(57) 4.87486(79)
The cell volume (nm^3)	0.56243(17)	0.68307(22)
Density (g/cm^3)	5.318(91)	5.36014(50)
R-Bragg (%)	0.873	0.428

Table. 3. Atomic positional parameters in $MnIn_2Se_4$

Atoms	Multiplicity of positions	*x*	*y*	*z*	Atom type	Relative occupation
In1	6	0.00000	0.00000	0.76964(31)	In^{+3}	1.000(42)
Se2	6	0.00000	0.00000	0.70467(46)	Se	1
Se1	6	0.00000	0.00000	0.12160(56)	Se	1
Mn	3	0.00000	0.00000	0.00000	Mn^{+2}	1.001(68)

Table.4. Atomic positional parameters in $Mn_2In_2Se_5$

Atoms	Multiplicity of positions	*x*	*y*	*z*	Atom type	Relative occupation
Se2	6	0.00000	0.00000	0.39354(22)	Se	1
Mn1	6	0.00000	0.00000	0.70092(31)	Mn^{+2}	1
Se1	6	0.00000	0.00000	0.13546(20)	Se	1
In2	6	0.00000	0.00000	0.55513(13)	In^{+3}	1
Se3	3	0.00000	0.00000	0.00000	Se	1

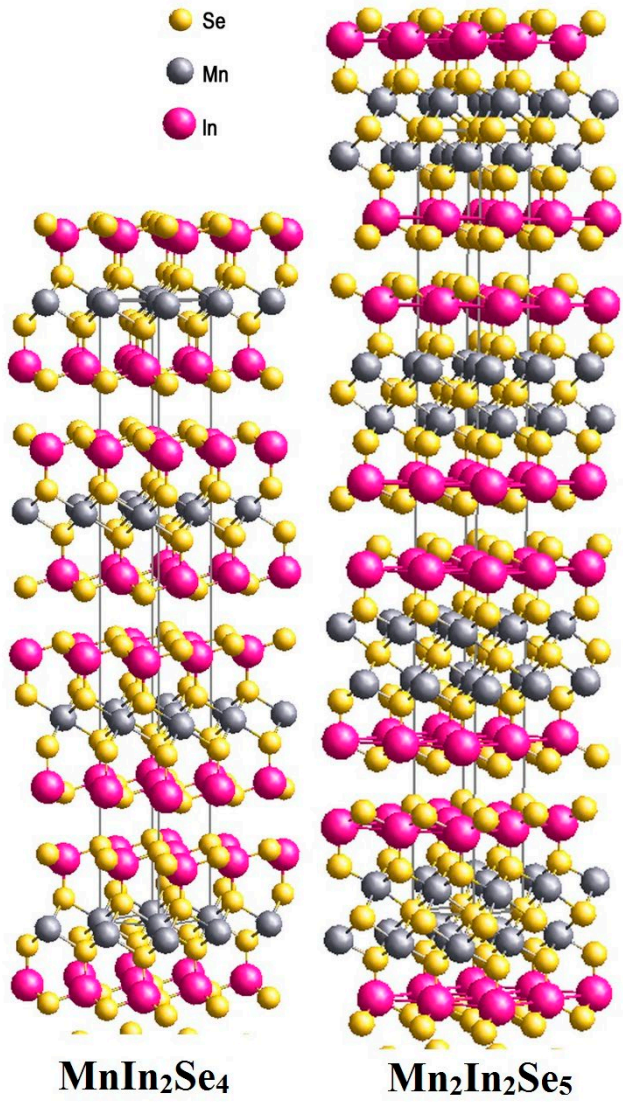

Fig. 4. Three-dimensional view of the structures of $MnIn_2Se_4$ and $Mn_2In_2Se_5$

It should be noted that the $MgIn_2Se_4$ and $ZnIn_2S_4$ compounds are also characterized by a similar structure, however, the authors [60] chose an asymmetric space group $R\bar{3}m$ to describe the structure of $MgIn_2Se_4$.

Interpretation of DTA data on the heating of annealed alloys of MnSe–In_2Se_3 system (Table 5), taking into account the above presented XRD results, allowed us to construct a *T-X* phase diagram (Fig. 5). According to our data, the MnSe–In_2Se_3 system can be considered quasi-binary, since the compositions of all phases in equilibrium are on its *T-X* planes. The system is characterized by the formation of two intermediate compounds: the $MnIn_2Se_4$ compound melts congruently at 1195 K and has a wide homogeneity region

Table. 5. DTA results of alloys of the MnSe–In_2Se_3 system

Composition, mol. % In_2Se_3	Thermal effects, K
10	–
20	1195
30	1197; 1197–1440
33.3	1196; 1196–1390
35	1188–1196; 1196–1360
40	1188 –1196; 1196-1285
45	1188
50	1195
55	1180–1193
60	1150–1190
70	462; 1148; 1148–1185
80	460; 1148; 1148–1176
90	463; 910; 1005; 1150
95	465; 910; 1005;1148–1155
100	475; 920 ; 1023; 1163

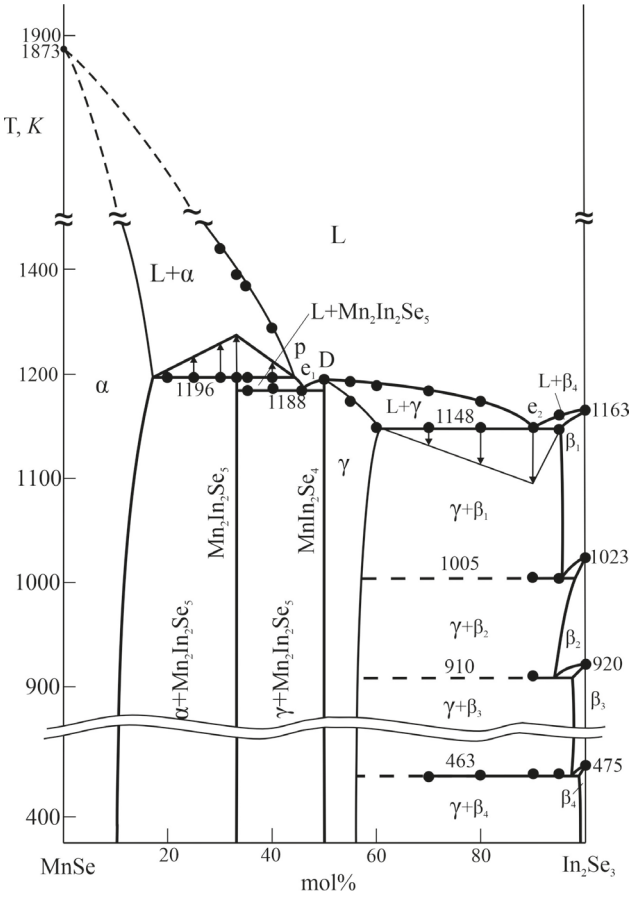

Fig. 5. Phase diagram of the MnSe-In_2Se_3 system

(γ-phase) towards an excess of the In_2Se_3. The second compound of the composition $Mn_2In_2Se_5$ melts with decomposition according to the peritectic reaction L + a ↔ $Mn_2In_2Se_5$ at 1196 K. The peritectic point has a composition of 42 mol. % In_2Se_3, the γ-phase is in eutectic equilibrium with the neighboring phases:

L ↔ $Mn_2In_2Se_5$ + γ
(point e_1, 45 mol. % In_2Se_3, 1188 K)
L ↔ β_1 + γ (point e_2, 90 mol. % In_2Se_3, 1148 K).

The compositions of the peritectic and eutectic points, as well as the homogeneity regions of the phases, were refined by the plotting of the Tamman's triangle (Fig. 5). It has been established that the homogeneity region of the α-phase at the peritectic temperature is 15 mol. %, and at eutectic temperature e_2 homogeneity regions of γ- and β_1-phases reach 10 and 5 mol. %, respectively. With a decreasing temperature of the homogeneity region the α- and γ-phases were somewhat narrowed and, according to X-ray diffraction data (Fig. 1), at room temperature, they were ~10 and 5 mol. %.

The phase compositions of the alloys, in particular the areas of phase homogeneity, were confirmed by SEM results (Fig. 6). As can be seen, the SEM images are in accordance with the phase diagram: the alloy with the composition 55 mol. % In_2Se_3, as well as the alloy with the stoichiometric composition $MnIn_2Se_4$ are single-phase, and the other three samples from different two-phase regions of the phase diagram are two-phase.

The obtained pattern of phase equilibria in the MnSe– In_2Se_3 system differed significantly from the data obtained in [51]. The phase diagram presented in [51] reflected only one ternary compound: $MnIn_2Se_4$ with congruent melting at ~1200 K. In

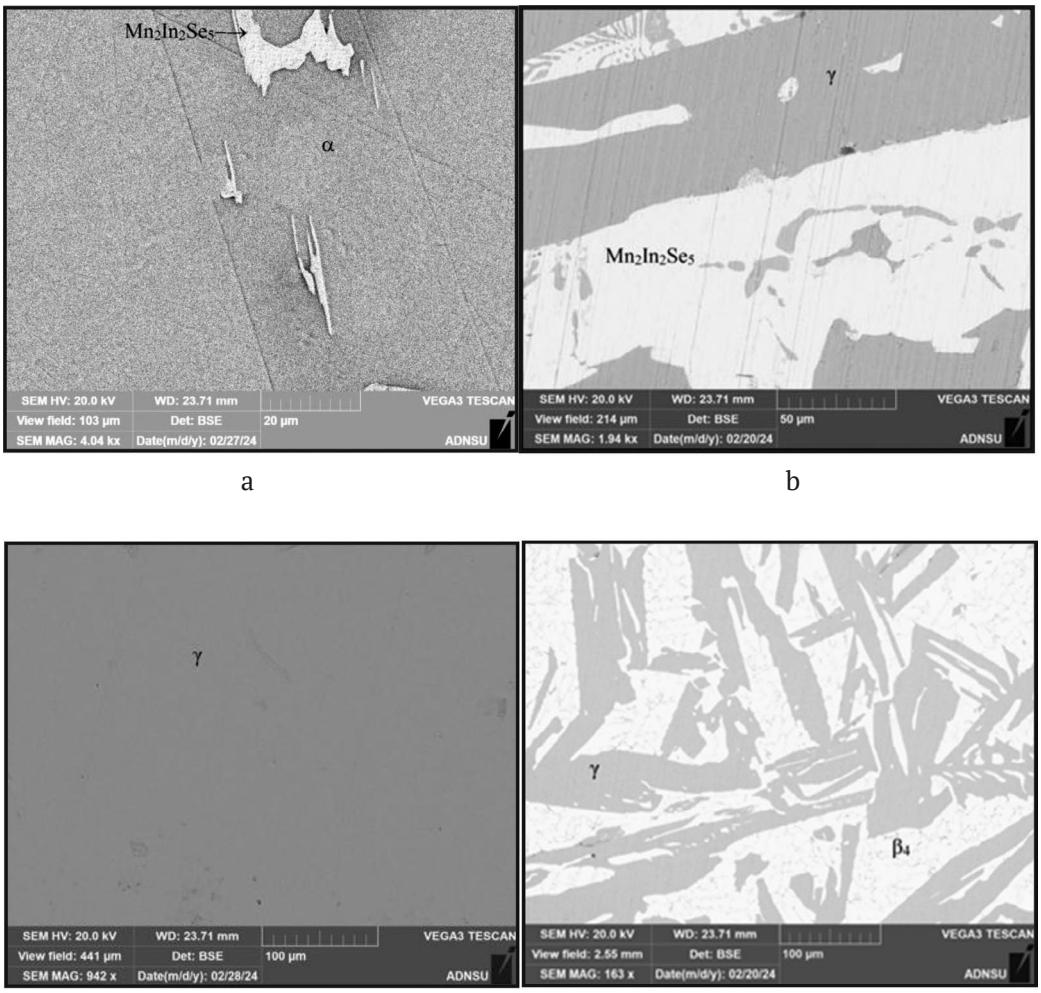

Fig. 6. SEM images of some single- and two-phase alloys of the MnSe-In_2Se_3 system: a) 15; b) 40; c) 55 and d) 70 mol. % In_2Se_3

addition, according to data [51], solubility based on MnSe was practically absent, and homogeneity regions based on various modifications of In_2Se_3 ranged from 5 (low temperature) to 25 mol. % (high temperature). Our data also differ significantly from data of [51] for the coordinates of eutectic and eutectoid equilibria.

4. Conclusions

Thus, we present a new refined version of the phase diagram of the MnSe-In_2Se_3 system, on which, in contrast to the data [51], in addition to $MnIn_2Se_4$, a ternary compound of the $Mn_2In_2Se_5$composition, melting with decomposition according to a peritectic reaction at 1196 K, was also formed. According to our data, $MnIn_2Se_4$ melts congruently at 1193 K and is a phase of variable composition, the homogeneity region at room temperature is ~5 mol. %. The crystal structures and lattice parameters of the $MnIn_2Se_4$ and $Mn_2In_2Se_5$ compounds were refined based on the XRD data, using the Rietveld method. Both ternary compounds were shown to have a layered structure and crystallize in the $R\bar{3}m$ space group.

Author contributions

F. M. Mammadov – research concept, discussion of results, writing the article; S. Z. Imamaliyeva – processing of the obtained results and participation in writing the article; E. N. Ismailova – literature search and participation in experiments; I. R. Amiraslanov – conducting structural studies; E. I. Akhmedov – processing the obtained results and writing the article; M. B. Babanly – scientific leadership, scientific editing.

Conflict of interests

The authors declare that they have no known competing financial interests or personal relationships that could have influenced the work reported in this paper.

References

1. Wyżga P., Veremchuk I., Bobnar M., Hennig C., Jasper A. L., Gumeniuk R. Ternary MIn_2S_4 (M = Mn, Fe, Co, Ni) thiospinels – crystal structure and thermoelectric properties. *Zeitschrift für anorganische und allgemeine Chemie*. 2020;646(14): 1091. https://doi.org/10.1002/zaac.202000014

2. Karthikeyan N., Aravindsamy G., Balamurugan P., Sivakumar K. Thermoelectric properties of layered type $FeIn_2Se_4$ chalcogenide compound. *Materials Research Innovations*. 2018;22(5): 278. https://doi.org/10.1080/14328917.2017.1314882

3. Hyunjung K., Tiwari A. P., Hwang E., ... Hyoyoung L. $FeIn_2S_4$ nanocrystals: a ternary metal chalcogenide material for ambipolar field-effect transistors. *Advanced Science*. 2018;5(7): 1800068. https://doi.org/10.1002/advs.201800068

4. Yang J., Zhou Z., Fang J., ... Wei Z. Magnetic and transport properties of a ferromagnetic layered semiconductor $MnIn_2Se_4$. *Applied Physics Letters*. 2019;115(22): 222101. https://doi.org/10.1063/1.5126233

5. Myoung B. R., Lim J. T., Kim C. S. Investigation of magnetic properties on spin-ordering effects of $FeGa_2S_4$ and $FeIn_2S_4$. *Journals of Magnetism and Magnetic Materials*. 2017;438: 121. https://doi.org/10.1016/j.jmmm.2017.04.056

6. Ranmohotti K. G. S., Djieutedjeu H., Lopez J., ... Poudeu P. F. P. Coexistence of high-T c herromagnetism and n-type electrical conductivity in $FeBi_2Se_4$. *Journal of the American Chemical Society*. 2015;137(2): 691–698. https://doi.org/10.1021/ja5084255

7. Guratinder K., Schmidt M., Walker H. C., ... Zharko O. Magnetic correlations in the triangular antiferromagnet $FeGa_2S_4$. Physical Review B. 2021;104: 064412. https://doi.org/10.1103/PhysRevB.104.064412

8. Romero L., Pacheco J., Cadenas R. Calculation of the lattice energy and the energy gap of the magnetic semiconductor $MnGa_2Se_4$ using Hartree-Fock and density functional theory methods. *Revista Mexicana de F´ısica*. 2016;62(6): 526–529. Режим доступа: https://www.scielo.org.mx/scielo.php?script=sci_arttext&pid=S0035-001X2016000600526

9. Verchenko V. Yu., Kanibolotskiy A.V., Bogach A. V., Znamenkova K. O., Shevelkov A. V. Ferromagnetic correlations in the layered van der Waals sulfide $FeAl_2S_4$. *Dalton Transactions*. 2022;51(21): 8454–8460. https://doi.org/10.1039/d2dt00671e

10. Hwang Y., Choi J., Ha Y., Cho S., Park H. Electronic and optical properties of layered chalcogenide $FeIn_2Se_4$. *Current Applied Physics*. 2020;20(1): 212–218. https://doi.org/10.1016/j.cap.2019.11.005

11. Pauliukavets S. A., Bychek I. V., Patapovich M. P. Specific features of the growth, structure, and main physicochemical properties of $FeGa_2Se_4$ single crystals. *Inorganic Materials: Applied Research*. 2018;9(2): 207–211. https://doi.org/10.1134/S2075113318020223

12. Chernoukhov I. V., Bogach A. V., Cherednichenko K. A., Gashigullin R. A., Shevelkov A. V., Verchenko V. Yu. $Mn_2Ga_2S_5$ and $Mn_2Al_2Se_5$ van der Waals chalcogenides: a source of atomically thin nanomaterials. *Molecules*. 2024;29(9): 12. https://doi.org/10.3390/molecules29092026

13. Verchenko Yu. V., Kanibolotskiy A.V., Chernoukhov I. V., ... Shevelkov A. V. Layered van der Waals chalcogenides $FeAl_2Se_4$, $MnAl_2S_4$, and $MnAl_2Se_4$: atomically thin triangular arrangement of transition-metal atoms. *Inorganic Chemistry*. 2023;62(19): 7557–7565. https://doi.org/10.1021/acs.inorgchem.3c00912

14. Otrokov M. M., Klimovskikh I. I., Bentmann H., ... Chulkov E. V. Prediction and observation of an antiferromagnetic topological insulator. *Nature*. 2019;576: 416–422. https://doi.org/10.1038/s41586-019-1840-9

15. Estyunin D. A., Klimovskikh I. I., Shikin A. M., ... Chulkov E. V. Signatures of temperature driven antiferromagnetic transition in the electronic structure of topological insulator $MnBi_2Te_4$. *Materials*. 2020;8(2): 021105(1-7). https://doi.org/10.1063/1.5142846

16. Jahangirli Z. A., Alizade E. H., Aliev Z. S., ... Chulkov E. V. Electronic structure and dielectric function of Mn-Bi-Te layered compounds. *Journal of Vacuum Science and Technology B*. 2019;37(6): 062910. https://doi.org/10.1116/1.5122702

17. Garnica M., Otrokov M., Aguilar P. C., ... Miranda R. Native point defects and their implications for the Dirac point gap at $MnBi_2Te_4$(0001). *npj Quantum Materials*. 2022;7(7): 1. https://doi.org/10.1038/s41535-021-00414-6

18. Yonghao Y., Xintong W., Hao L., ... Qi-Kun X. Electronic states and magnetic response of $MnBi_2Te_4$ by scanning tunneling microscopy and spectroscopy. *Nano Letters*. 2020;20: 3271–3277. https://doi.org/10.1021/acs.nanolett.0c00031

19. Zhou L., Tan Z., Yan D., Fang Z., Shi Y., Weng H. Topological phase transition in the layered magnetic compound $MnSb_2Te_4$: spin-orbit coupling and interlayer coupling dependence. *Physical Review B*. 2020;102: 085114(1-8). https://doi.org/10.1103/PhysRevB.102.085114

20. Zhu T., Bishop A. J., Zhou T. Synthesis, magnetic properties, and electronic structure of magnetic topological insulator $MnBi_2Se_4$. *Nano Leterst*. 2021;21(12): 5083–5090. https://doi.org/10.1021/acs.nanolett.1c00141

21. Swatek P., Wu Y., Wang L. L. Gapless Dirac surface states in the antiferromagnetic topological insulator $MnBi_2Te_4$. *Physical Review B: Condensed Matter and Materials Physics*. 2020;101(16): 161109. https://doi.org/10.1103/PhysRevB.101.161109

22. Ovchinnikov D., Huang X., Lin Z., ... Xu X. Intertwined topological and magnetic orders in atomically thin chern insulator $MnBi_2Te_4$. *Nano Letters*. 2021;21(6): 2544. https://doi.org/10.1021/acs.nanolett.0c05117

23. Liang H., Feng T., Tan S., ... Cao L. Two-dimensional (2D) $MnIn_2Se_4$ nanosheets with porous structure: a novel photocatalyst for water splitting without sacrificial agents. *Chemical Communications*. 2019;55: 15061. https://doi.org/10.1039/C9CC08145C

24. Chen W., He Z. C., Huang G. B., Wu C.-L., Chen W.-F., Liu X.-H. Direct Z-scheme 2D/2D $MnIn_2S_4$/g-C_3N_4 architectures with highly efficient photocatalytic activities towards treatment of pharmaceutical wastewater and hydrogen evolution. *Chemical Engineering Journal*. 2019;359: 244. https://doi.org/10.1016/j.cej.2018.11.141

25. Song Y., Guo Y., Qi S., ... Lou Y. Cu_7S_4/$MnIn_2S_4$ heterojunction for efficient photocatalytic hydrogen generation. *Journal of Alloys and Compounds*. 2021;884: 161035. https://doi.org/10.1016/j.jallcom.2021.161035

26. Zhang B., Liu Y., Zhu H., Gu D., Zhou K., Hao J. Enhanced visible light photocatalytic performance of a novel $FeIn_2S_4$ microsphere/BiOBr nanoplate heterojunction with a Z-scheme configuration. *Environmental Science and Pollution Research*. 2023;30: 13438–13448 . https://doi.org/10.1007/s11356-022-22929-6

27. Sharan A., Sajjad M., Singh D. J., Singh N. Two-dimensional ternary chalcogenides FeX2Y4 (X = Ga, In; Y = S, Se, Te): Promising materials for sustainable energy. *Physical Review Materials*. 2022;6: 094005. https://doi.org/10.1103/PhysRevMaterials.6.094005

28. Muruganantham R., Chen J.-A., Yang C.-C. Spinel phase $MnIn_2S_4$ enfolded with reduced graphene oxide as composite anode material for lithium-ion storage. *Materials Today Sustainability*. 2023;21: 100278. https://doi.org/10.1016/j.mtsust.2022.100278

29. Wu P., Huang Ch., Hsieh Ch., Liu W. Synthesis and characterization of $MnIn_2S_4$/single-walled carbon nanotube composites as an anode material for lithium-ion batteries. *Nanomaterials*. 2024;14(18): 716. https://doi.org/10.3390/nano14080716

30. Yan D., Li K., Yan Y., ... Yang H. Y. Cubic spinel XIn_2S_4 (X = Fe, Co, Mn): a new type of anode material for superfast and ultrastable Na-ion storage. *Advanced Energy Materials*. 2021;11: 2102137. https://doi.org/10.1002/aenm.202102137

31. Tarasov A. V., Makarova T. P., Estyunin D. A., ... Shikin A. M. Topological phase transitions driven by Sn doping in $(Mn_{1-x}Sn_x)Bi_2Te_4$. *Symmetry*. 2023;15(2): 469. https://doi.org/10.3390/sym15020469

32. Djieutedjeu H., Lopez J. S., Lu R., ... Poudeu P. F. P. Charge disproportionation triggers bipolar doping in $FeSb_{2-x}Sn_xSe_4$ ferromagnetic semiconductors, enabling a temperature-induced lifshitz transition. *Journal of the American Chemical Society*. 2019;141(23): 9249. https://doi.org/10.1021/jacs.9b01884

33. Levy I., Forrester C., Ding X., Testelin C., Krusin-Elbaum L., Tamargo M. C. High Curie temperature ferromagnetic structures of $(Sb_2Te_3)_{1-x}(MnSb_2Te_4)_x$ with $x = 0.7–0.8$. *Scientific Reports*. 2023;13: 7381. https://doi.org/10.1038/s41598-023-34585-y

34. Moroz N. A., Lopez J. S., Djieutedjeu H., ... Poudeu P. F. P. Indium preferential distribution enables electronic engineering of magnetism in $FeSb_{2-x}In_xSe_4$ *p*-type high-Tc ferromagnetic semiconductors. *Chemistry of Materials*. 2016;28(23): 8570. https://doi.org/10.1021/acs.chemmater.6b03293

35. Levy I., Forrester C., Deng H., ... Tamargo M. C. Compositional control and optimization of molecular beam epitaxial growth of $(Sb_2Te_3)_{1-x}(MnSb_2Te_4)_x$ magnetic topological insulators. *Crystal Growth and Design*. 2022;22(5): 3007. https://doi.org/10.1021/acs.cgd.1c01453

36. Liu Y., Kang Ch., Stavitski E., Attenkofer K., Kotliar G., Petrovic C. Polaronic transport and thermoelectricity in $Fe_{1-x}Co_xSb_2S_4$ (x = 0, 0.1, and 0.2). *Physical Review B*. 2018;97(15): 155202. https://doi.org/10.1103/PhysRevB.97.155202

37. Babanly M. B., Yusibov Y. A., Imamaliyeva S. Z., Babanly D. M., Alverdiyev I. J. Phase diagrams in the development of the argyrodite family compounds and solid solutions based on them. *Journal of Phase Equilibria and Diffusion*. 2024;45: 228–255 https://doi.org/10.1007/s11669-024-01088-w

38. Babanly M. B., Mashadiyeva L. F., Imamaliyeva S. Z., Tagiev D. B., Babanly D. M., Yusibov Yu. A. Thermodynamic properties of complex copper chalcogenides (review). *Chemical Problems*. 2024;3(22): 243-280. https://doi.org/10.32737/2221-8688-2024-3-243-280

39. Imamaliyeva S. Z., Mekhdiyeva I. F., Babanly D. M., Zlomanov V. P., Tagiyev D. B., Babanly M. B. Solid-phase equilibria in the $Tl_2Te–Tl_2Te_3–TlErTe_2$ system and the thermodynamic properties of the Tl_9ErTe_6 and $TlErTe_2$ compounds. *Russian Journal of Inorganic Chemistry*. 2020;65: 1762–1769. https://doi.org/10.1134/S0036023620110066

40. Orujlu E. N., Aliev Z. S., Babanly M. B. The phase diagram of the $MnTe–SnTe–Sb_2Te_3$ ternary system and synthesis of the iso- and aliovalent cation-substituted solid solutions. *Calphad*. 2022;76: 102398. https://doi.org/10.1016/j.calphad.2022.102398

41. Aghazade A. I., Babanly D. M., Zeynalova G. S., Gasymov V. A., Imamaliyeva S. Z. Phase relations in the Bi_2-Bi_2Se_3-Bi_2Te_3 system and characterization of solid solutions. *Azerbaijan Chemical Journal*. 2024;1: 76–88. https://doi.org/10.32737/0005-2531-2024-76-88

42. Ismailova E.N., Mashadiyeva L.F., Bakhtiyarly I.B., Babanly M.B. Phase equilibria in the Cu2SnSe3–Sb2Se3–Se system. *Condensed Matter and Interphases*. 2023; 25(1): 47–54 https://doi.org/10.17308/kcmf.2023.25/10973

43. Mammadov S. H. The study of the quasi-triple system FeS-Ga_2S_3-Ag_2S by a $FeGa_2S_4$-$AgGaS_2$ section. *Condensed Matter and Interphases.* 2020;22(2): 232–237.

44. Mammadov F. M., Imamaliyeva S. Z., Jafarov Ya. I., Bakhtiyarly I. B., Babanly M. B. Phase equilibria in the MnTe–$MnGa_2Te_4$–$MnIn_2Te_4$ system. *Condensed Matter and Interphases*. 2022;24(3): 335–344. https://doi.org/10.17308/kcmf.2022.24/9856

45. Mammadov F. M., Amiraslanov I. R., Imamaliyeva S. Z., Babanly M. B. Phase relations in the FeSe–$FeGa_2Se_4$–$FeIn_2Se_4$ system: refinement of the crystal structures of $FeIn_2Se_4$ and $FeGaInSe_4$. *Journal of Phase Equilibria and Diffusion*. 2019;40(6): 787–796. https://doi.org/10.1007/s11669-019-00768-2

46. Mammadov F. M., Agayeva R. M., Amiraslanov I. R., Babanly M. B. Revised phase diagram of the MnSe–Ga_2Se_3 system. *Russian Journal of Inorganic Chemistry.* 2024. https://doi.org/10.1134/S0036023623602611

47. Mamedov F. M., Babanly D. M., Amiraslanov I. R., Tagiev D. B., Babanly M. B. Physicochemical analysis of the FeSe–Ga2Se3–In2Se3 system. *Russian Journal of Inorganic Chemistry*. 2020;65(11): 1747–1755. https://doi.org/10.1134/s0036023620110121

48. Mammadov F. M., Amiraslanov I. R., Aliyeva Y. R., Ragimov S. S., Mashadiyeva L. F., Babanly M. B. Phase equilibria in the $MnGa_2Te_4$-$MnIn_2Te_4$ system, crystal structure and physical properties of $MnGaInTe_4$. *Acta Chimica Slovenica.* 2019;66: 466. https://doi.org/10.17344/acsi.2019.4988

49. Mammadov F. M., Babanly D. M., Amiraslanov I. R., Tagiev D. B., Babanly M. B. FeS–Ga_2S_3–In_2S_3 system. *Russian Journal of Inorganic Chemistry*. 2021;66(10): 1533. https://doi.org/10.1134/s0036023621100090

50. Mammadov F. M., Niftiev N. N., Jafarov Ya. I., Babanly D. M., Bakhtiyarly I. B., Babanly M. B. Physicochemical analysis of the MnTe–Ga_2Te_3–In_2Te_3 system and AC electrical conductivity of $MnGaInTe_4$. *Russian Journal of Inorganic Chemistry*. 2022;67(10): 1623–1633. https://doi.org/10.1134/S0036023622600769

51. Babaeva P. K., Allazov M. R. *Research in the field of inorganic and physical chemistry**. Collection of works / Z. G. Zulfugarov et al. (eds.). Institute of Inorganic and Physical Chemistry of the USSR Academy of Sciences. Baku: Elm, 1974. 318 p. (In Russ.)

52. *Phase diagrams of binary metallic systems** / N. R. Lyakishev (rd.). Moscow: Mashinostroenie Publ.; 2001. Vol. 3. Book 1. p. 382.

53. Massalski T. B. *Binary alloy phase diagrams - second edition*.,Ohio: ASM International Materials Park; 1990. 3875 p.

54. Hussain R. A., Hussain I. Manganese selenide: synthetic aspects and applications. *Journal of Alloys and Compounds*. 2020;842(25): 155800. https://doi.org/10.1016/j.jallcom.2020.155800

55. Hyunjung K.,Vogelgesang R., Ramdas A. K., Peiris F. C., Bindley U., Furdyna J. K. MnSe: rocksalt versus zinc-blende structure. *Physical Review B*. 1998;58(11): 6700–6703. https://doi.org/10.1103/physrevb.58.6700

56. Jiping Ye J. Y., Sigeo Soeda S. S., Yoshio Nakamura Y. N., Osamu Nittono O. N. Crystal structures and phase transformation in In_2Se_3 compound semiconductor. *Japanese Journal of Applied Physics.* 1998; 37(8R): 4264. https://doi.org/10.1143/JJAP.37.4264

57. Emsley J. *The elements*. Oxford University Press; 1998. 300 p.

58. Range K.-J., Klement U., Döll G. Notizen: The crystal structure of $MnIn_2Se_4$, a ternary layered semiconductor. *Zeitschrift Für Naturforschung B*. 1991;46(8): 1122. https://doi.org/10.1515/znb-1991-0825

59. Range K.-J., Klemnt U., Döll G. Dimanganese diindium pentaselenide, $Mn_2In_2Se_5$. *Acta Crystallographica Section C Crystal Structure Communications*. 1992;48(2): 355 https://doi.org/10.1107/S0108270191008521

60. Dotzel P., Schäfer H., Schön G. Zur Darstellung und Strukturchemie Ternärer Selenide des Magnesiums mit Indium und Aluminium. *Zeitschrift für anorganische und allgemeine Chemie*. 1976;426: 260-268. https://doi.org/10.1002/zaac.19764260305

** Translated by author of the article*

Information about the authors

Faik M. Mammadov, PhD (Chem.), Assistance Professor, Leading Researcher, Institute of Catalysis and Inorganic Chemistry (Baku, Azerbaijan).
https://orcid.org/0000-0003-3317-7438
faikmamadov@mail.ru

Samira Z. Imamaliyeva, Dr. Sci. (Chem.), Assistance Professor, Institute of Catalysis and Inorganic Chemistry (Baku, Azerbaijan).
https://orcid.org/0000-0001-8193-2122
samira9597a@gmail.com

Elnara N. Ismailova, PhD student, Researcher, Institute of Catalysis and Inorganic Chemistry (Baku, Azerbaijan).
https://orcid.org/0000-0002-1327-1753
ismayilova818@mail.ru

Imamaddin R. Amiraslanov, Dr. Sci. (Phys.), Professor, Head of Laboratory, Institute of Physics (Baku, Azerbaijan).
https://orcid.org/0000-0001-7975-614X
iamiraslan@gmail.com

Eldar I. Ahmadov, Dr. Sci. (Chem.), Professor, Baku State University (Baku, Azerbaijan).
eldar_akhmedov@mail.ru

Mahammad B. Babanly, Dr. Sci. (Chem.), Professor, Associate Member of the Azerbaijan National Academy of Sciences, Deputy-director of the Institute of Catalysis and Inorganic Chemistry (Baku, Azerbaijan).
https://orcid.org/0000-0001-5962-3710
babanlymb@gmail.com

Received 05.09.2024; approved after reviewing 18.09.2024; accepted for publication 15.10.2024; published online 25.03.2025.

Translated by Valentina Mittova